Research Article
doi: 10.1590/01047760202632013736
vol(32), 2026

CERNE

Technical and environmental performance of particleboards from *Erythrina poeppigiana* (Walp.) O.F. Cook in agroforestry systems

Lívia Berti Sanjuan Farias[1], José Adolfo de Almeida Neto[2], Ricardo Gabriel de Almeida Mesquita[3], Daniel Piotto[3], Mara Lúcia Agostini Valle[3], José Benedito Guimarães Junior[4], Lourival Marin Mendes[4].

[1] Federal University of Southern Bahia, Rector's Office, Itabuna, BA, Brazil.
[2] Department of Agricultural and Environmental Sciences, State University of Santa Cruz, Salobrinho, Ilhéus, BA, Brazil.
[3] Federal University of Southern Bahia, Center for Training in Agroforestry Sciences, Brazil.
[4] Federal University of Lavras, Department of Forest Sciences, Brazil.

TECHNOLOGY OF FOREST PRODUCTS

ABSTRACT

Background: This study evaluated the technical performance, energy demand, and carbon footprint of particleboards produced from *Erythrina poeppigiana* (Walp.) O.F. Cook wood obtained from agroforestry systems, considering different panel densities and structural configurations.

Results: Panel density significantly influenced both physical properties and environmental performance. Single-layer panels showed improved dimensional stability, with thickness swelling values below 22%, whereas multilayer panels exceeded this limit. Water absorption ranged from 40.1 to 78.4%, confirming the high hygroscopicity of the material. Mechanical performance was satisfactory, with modulus of elasticity ranging from 2062 to 2654 MPa, while modulus of rupture (18.6–23.7 MPa) and internal bond strength (0.49–0.80 MPa) showed no significant differences among treatments. In the cradle-to-gate assessment, energy demand ranged from 4649 to 4869 $MJ \cdot m^{-3}$ and CO_2e emissions from 189.89 to 203.06 kg $CO_2e \cdot m^{-3}$. Lower-density panels showed the lowest environmental impacts due to reduced wood and adhesive consumption. Adhesive production was the main contributor, accounting for approximately 72–74% of total emissions.

Conclusions: *E. poeppigiana* wood from agroforestry systems is a viable alternative raw material for particleboard production. Panel structure and material efficiency were the main factors controlling performance and environmental impacts. High water absorption values (40.1–78.4%) represent a critical limitation, compromising dimensional stability and restricting multilayer configurations under moisture exposure. Improvements in dimensional stability are still required.

Keywords: *Biomass valorization; Cabruca; Carbon footprint; Dimensional stability; Urea–formaldehyde.*

HIGHLIGHTS

Single-layer panels showed lower thickness swelling than multilayer panels
MOE varied, while MOR and IB remained stable
Lower density reduced CO_2e emissions by up to 6.5%
UF adhesive accounted for ~72–74% of total emissions

FARIAS, L. B. S.; ALMEIDA NETO, J. A.; MESQUITA, R. G. A.; PIOTTO, D.; VALLE, M. L. A.; GUIMARÃES JUNIOR, J. B.; MENDES, L. M. Technical and environmental performance of particleboards from Erythrina poeppigiana (Walp.) O.F. Cook in agroforestry systems. CERNE, v. 32, e103736, 2026. DOI: 10.1590/01047760202632013736.

✤Corresponding author: ricardo.mesquita@ufsb.edu.br
Scientific Editor: Paulo Ricardo Gherardi Hein

Received: April 30 2026
Accepted: May 26 2026

CERNE
ISSN 0104-7760
UNIVERSIDADE FEDERAL DE LAVRAS

INTRODUCTION

Cacao-based agroforestry systems in southern Bahia, Brazil, such as the cabruca system, combine agricultural production with biodiversity conservation and ecosystem services (Gama-Rodrigues *et al.*, 2021). In these systems, *Erythrina* species are commonly used as shade trees, regulating microclimatic conditions for cocoa cultivation (Gama-Rodrigues *et al.*, 2021). Agroforestry systems, however, remain underutilized as sources of lignocellulosic raw materials, despite their potential for timber production (Piotto *et al.*, 2020).

The valorization of *Erythrina poeppigiana* as a lignocellulosic resource represents an opportunity to integrate material use with agroforestry systems, contributing to raw material diversification and to the use of underutilized biomass, improving resource efficiency in wood-based systems (Costa *et al.*, 2024). This perspective is relevant considering the Brazilian wood-based panel industry, which stands out globally due to its high productivity and growing demand (IBÁ, 2025). The sector is recognized as a reference in large-scale bioeconomy based on renewable resources, yet it remains strongly dependent on species of the genus Pinus, which are geographically concentrated. This dependence creates potential supply constraints and may increase production costs, reinforcing the need to investigate alternative lignocellulosic resources capable of diversifying the industrial base (Corrêa *et al.*, 2025; Lourenço *et al.*, 2025).

Among potential alternatives, *E. poeppigiana* has been studied for panel production, particularly in plywood and wood-cement systems, demonstrating technical feasibility. These applications, however, generally present lower mechanical performance, especially in terms of stiffness, due to the low density of the material (Farias *et al.*, 2024; Custódio *et al.*, 2025; Mesquita *et al.*, 2026). However, information on the use of this species for particleboard (MDP) production remains limited, particularly when both technical and environmental performance are considered.

This limitation is associated with the intrinsic relationship between wood density and mechanical properties, in which lower-density materials tend to exhibit reduced modulus of elasticity and strength. Densification is a promising strategy to enhance the performance of low-density lignocellulosic materials. The process reduces voids and increases material density, improving mechanical strength, stiffness, and dimensional stability (Cabral *et al.*, 2022; Luan *et al.*, 2022). The use of *E. poeppigiana* in particleboard production may therefore overcome its natural limitations, as panel densification during pressing can improve structural performance.

Considering the use of *E. poeppigiana* in cocoa agroforestry systems in southern Bahia (Gama-Rodrigues *et al.*, 2021), its industrial utilization represents a strategic opportunity. It may add value to underutilized biomass, generate additional income for producers, and promote more efficient use of available biomass within these systems (Farias *et al.*, 2024; Costa *et al.*, 2024). The rational management of shading species can also contribute to biodiversity conservation by improving ecological balance.

From an industrial perspective, evaluating both technical and environmental performance is essential, as improvements in material properties may influence energy demand and resource efficiency (Costa *et al.*, 2024; Mohd Azman *et al.*, 2021). This study evaluated the technical feasibility, energy demand, and carbon footprint of particleboards produced from *E. poeppigiana* wood, using a cradle-to-gate inventory focused on energy consumption and CO_2e emissions. Simplified cradle-to-gate environmental inventories focused on energy demand and CO_2e emissions have been increasingly applied to wood-based panels as practical tools for comparing material efficiency and identifying opportunities for environmental improvement (Costa *et al.*, 2024; Mohd Azman *et al.*, 2021).

Although *E. poeppigiana* has already been investigated for plywood and wood-cement applications, studies integrating the technical performance of particleboards with simplified environmental indicators remain scarce. The main novelty of the present study lies in the combined evaluation of panel performance and cradle-to-gate environmental indicators (energy demand and CO_2e emissions) for particleboards produced from this agroforestry species. Recent studies have demonstrated that the integration of mechanical performance and environmental indicators through LCA can support the identification of more eco-efficient materials for particleboard production (Gavioli *et al.*, 2025).

Based on this gap, the hypothesis of this study is that particleboards produced from *E. poeppigiana* can achieve physical and mechanical properties compatible with standard requirements through densification during panel pressing, while presenting competitive environmental performance in terms of energy demand and CO_2e emissions when compared to conventional raw materials.

MATERIAL AND METHODS

Wood Harvesting and Preparation

The trees were harvested at the Jorge Amado Campus of the Federal University of Southern Bahia (UFSB), located between the coordinates 14°45′11.69″–14°47′6.84″ S and 39°14′17.27″–39°12′53.26″ W, within a cocoa-based agroforestry system estimated to be over 40 years old. *E. poeppigiana* trees were established vegetatively (from cuttings) alongside cacao and banana in the late 1980s, at a spacing of 12 × 12 m (approximately 70 trees ha^{-1}). Following establishment, the trees were allowed to grow freely to provide shade for the cacao. Tree selection was carried out randomly; only individuals with diameters compatible with veneer lathe processing were considered.

Four *E. poeppigiana* trees (average diameter of approximately 45 cm) were felled and converted into six 4-m logs. All material was obtained from the same agroforestry area to ensure consistency. The logs were transported by road using a conventional diesel-powered truck (two-axle) over a distance of approximately 1698 km, from Ilhéus (BA) to the Federal University of Lavras (MG), where they were processed.

Wood and Adhesive Characterization

Chemical analyses (lignin, extractives, and ash content) were conducted in accordance with NBR 7989 (ABNT, 2010), NBR 14853 (ABNT, 2010), and NBR 13999 (ABNT, 2017). Holocellulose content was calculated by difference. The basic wood density was determined in accordance with ABNT NBR 11941 (ABNT, 2003). Samples were obtained from discs collected at breast height (1.3 m from the ground). From each disc, wedge-shaped specimens were prepared to ensure representativeness of the cross-section. Four specimens were collected per tree. The basic density was calculated for each specimen, and the mean value per tree was used for analysis. Results are presented as mean ± standard deviation.

A commercial urea–formaldehyde (UF) adhesive (Redemite®) was used, acquired from the local market. Contact angle, viscosity, and solids content were evaluated (three replicates). The wettability of the adhesive was assessed through contact angle measurements using a goniometer (Krüss GmbH, Germany) coupled with ADVANCE software. A droplet of adhesive was deposited onto the surface of an *E. poeppigiana* strand, and the sessile drop method was applied to monitor its behavior. Image acquisition started immediately after deposition and was recorded over a period of 1 s. The contact angle was calculated as the mean value obtained within this initial time interval. All tests were conducted on strand surfaces previously conditioned at 22 ± 2 °C and 65 ± 5% relative humidity. Viscosity was determined using a Ford Cup No. 4 viscometer (ASTM D1200-10, 2018). Solids content was determined by drying 1 g of adhesive at 103 ± 3 °C for 3 h.

A urea–formaldehyde (UF) adhesive was used in this study, which is widely applied in the industrial production of particleboards. The objective was to evaluate the technical and environmental performance of the raw material under conventional manufacturing conditions. The results may support future studies focusing on the use of bio-based or low-emission adhesive systems.

Panel Manufacturing

Sliver-type particles were produced in a hammer mill and classified between 12 and 40 mesh. Fine particles were used for the surface layers and coarse particles for the core layer (three-layer panels). The particles were oven-dried at 80 °C until reaching constant mass, and the final moisture content was adjusted to 4%.

UF adhesive was applied in a rotary drum blender at 12% for the surface layers and 9% for the core (MDP panels). Treatment T4 (conventional particleboard) was manufactured as a single-layer panel with 10% UF adhesive.

The mats were formed in a mold (48 × 48 cm) at a proportion of 20% top surface, 60% core, and 20% bottom surface. Pre-pressing was performed at 4 tons, followed by hot pressing (3.92 MPa; 150 °C; 10 min). After pressing, panels were conditioned at 22 ± 2 °C and 65 ± 5% relative humidity.

Four treatments were produced with three replicates each. Processing conditions are presented in Table 1.

Table 1: Processing conditions and evaluated treatments.

Treatments	Structure	Nominal density ($g \cdot cm^{-3}$)	Time (min)	Temperature (°C)	Pressure (MPa)
T1	Three-layer	0.75	10	150	3.92
T2	Three-layer	0.72	10	150	3.92
T3	Three-layer	0.69	10	150	3.92
T4*	Single-layer	0.75	10	150	3.92

*T4: Conventional particleboard, single-layer, 10% UF resin.

Physical and Mechanical Characterization

After conditioning, the panels were trimmed and specimens were prepared for physical and mechanical testing. Apparent density, water absorption (WA2h and WA24h), thickness swelling (TS2h and TS24h), modulus of elasticity (MOE), and modulus of rupture (MOR) were determined in accordance with ASTM D1037 (2006).

Six specimens per panel were used for apparent density, water absorption, thickness swelling, and compaction ratio. For bending properties (MOE and MOR), two specimens per panel were tested. Internal bond strength (IB) was determined according to ABNT NBR 14810-2 (ABNT, 2024), using five specimens per panel.

The compaction ratio was calculated as the ratio between panel density and wood basic density, according to Iwakiri and Trianoski (2020).

The experimental procedure and equipment used for particleboard production and characterization are presented in Supplementary Figure S1.

Statistical Analysis

Three panels were produced for each treatment, and each panel was considered the experimental unit. Multiple specimens were obtained from each panel for physical and mechanical characterization; however, the mean value per panel was used in the statistical analysis to avoid pseudo-replication.

The results were subjected to the Shapiro–Wilk test to assess normality and the Levene test to verify homogeneity of variances, followed by analysis of variance (ANOVA). When significant differences were detected, Tukey's test ($p < 0.05$) was applied. All statistical analyses were performed using R software (R Core Team), adopting a 95% confidence level.

Inventory Analysis and System Definition

Figure 1 presents a simplified process flow of MDP production, including forestry operations and industrial

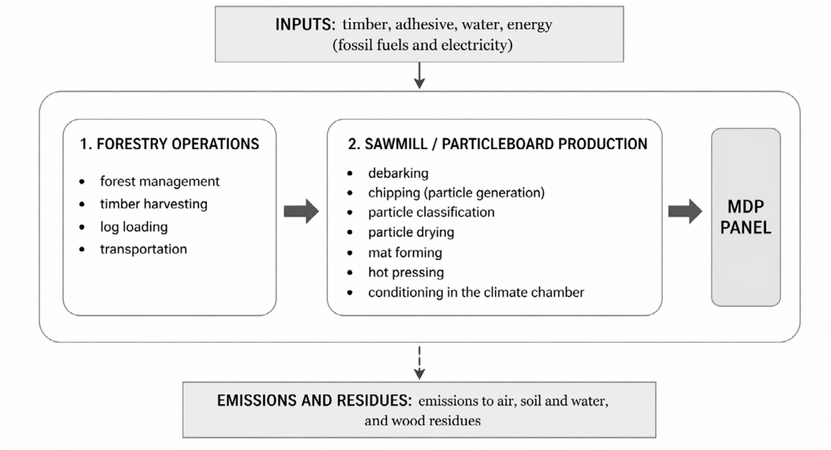

Figure 1: MDP production system by subsystem. Illustrative scheme.

processing stages. The main inputs (timber, adhesive, water, and energy) and outputs (emissions to air, water, and solid residues) are indicated along the production chain. Illustrative schemes were developed with the assistance of artificial intelligence tools (ChatGPT, OpenAI) and subsequently refined using CorelDRAW software.

The declared unit was 1 m^3 of MDP. The system boundary was defined as cradle-to-gate, encompassing wood extraction from agroforestry systems (AFS) to laboratory-scale panel production.

The system boundaries were defined considering two main subsystems: forest operations and industrial processing (Figure 2). The forest operation subsystem (Figure 2A) comprises biomass supply, including harvesting and log transportation. The industrial subsystem (Figure 2B) represents the processing of logs into particleboards (MDP), encompassing the main production stages from raw material conversion to panel conditioning.

The reference scenario considered the installation of an MDP plant in Ilhéus (BA), with a 50-km supply radius. Although laboratory production was conducted at the Federal University of Lavras (UFLA), the environmental inventory considered a hypothetical industrial-scale production scenario located in Ilhéus (BA), where the wood was harvested from a cocoa-based agroforestry system at the UFSB experimental farm. The southern Bahia region was considered representative due to the regional availability of *E. poeppigiana* biomass associated with cacao agroforestry systems. Transportation distances for input materials are presented in Table 2.

Energy Demand and CO_2e Emissions Calculation

Diesel consumption was calculated according to Equation 1:

$$C_{diesel} = D \times fc \quad (1)$$

where C_{diesel} is diesel consumption (L), D is the transport distance (km), and fc is the fuel consumption factor ($L \cdot km^{-1}$).

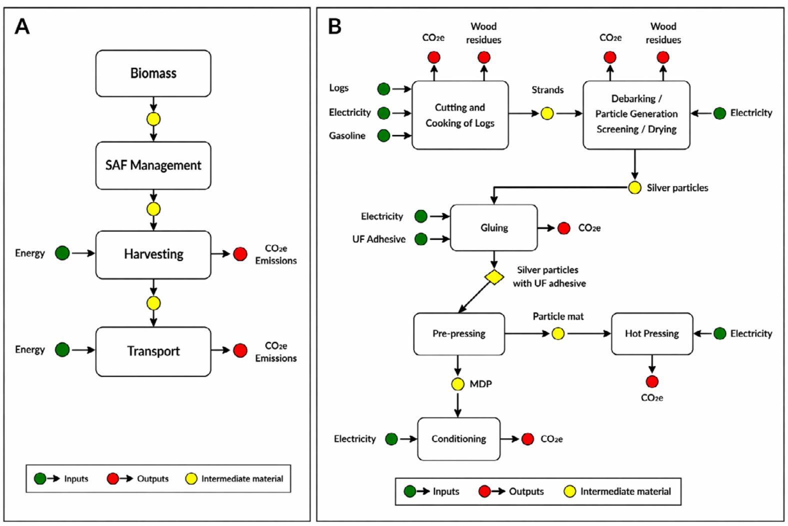

Figure 2: System boundaries and process flows for MDP production: (A) Forest operation subsystem, indicating biomass supply stages and associated inputs and emissions. (B) Industrial subsystem, detailing the main unit processes, material and energy flows, and outputs considered in the system. Illustrative scheme.

Table 2. Transport distance of input materials (Brazil)

Input Material	City of Origin	Destination City	Distance (km)	Diesel Consumption (L/km)	Total Diesel Consumption (L)	Specific Diesel Consumption (L/t)
Wood	Ilhéus (BA)	Ilhéus (BA)	50	0.42	21	0.0014
Urea-formaldehyde	São Paulo (SP)	Ilhéus (BA)	1697.5	0.42	712.95	0.04753

Fuel conversion into embodied energy was based on the factors presented in Table 3.

Table 3: Conversion of fuels into embodied energy.

Unit	Diesel oil (pure)	Biodiesel	Gasoline	Anhydrous ethanol
$MJ{\cdot}L^{-1}$	35.52	33.16	32.31	22.35

Source: Adapted from GHG Protocol (2022).

Emission factors for CO_2-equivalent (CO_2e) and energy demand used in the calculations are presented in Table 4.

Table 4: CO_2e emissions and energy demand

Flows	Unit	CO_2e Emissions (kg/unit)	Source	Energy Demand (MJ/unit)
Wood	m^3	0	Planted wood, biogenic CO_2	-
Gasoline	L	2.20	Emission factor from the National Greenhouse Gas Inventory (top-down approach)	29.62
Diesel oil	L	2.60	Emission factor from the National Greenhouse Gas Inventory (top-down approach)	35.21
Electricity	kWh	0.075	CO_2 emission factor for electricity generation in the Brazilian National Interconnected System (SIN) – Brasil (2019 average). Energy data: National Energy Balance (2018).	4.92

Simplified Cradle-to-Gate Environmental Assessment

A simplified cradle-to-gate environmental assessment was conducted following the framework proposed by Cabeza *et al.* (2014), based on system boundary definition, inventory analysis, impact assessment, and interpretation. In this study, a cradle-to-gate approach was adopted, focusing on the quantification of material and energy flows associated with particleboard production. The assessment was simplified to include only energy demand and CO_2-equivalent emissions, without considering additional impact categories. Therefore, the present study should not be interpreted as a complete life cycle assessment, but rather as a partial environmental assessment focused on energy demand and CO_2-equivalent emissions.

RESULTS

Wood and Adhesive Properties

The wood presented the following chemical composition (mean ± standard deviation): holocellulose (68.43 ± 0.83%), cellulose (43.01 ± 1.53%), lignin (18.91 ± 1.03%), extractives (9.54 ± 1.36%), and mineral content (3.12 ± 0.07%).

The basic density of *E. poeppigiana* was $0.26\ g{\cdot}cm^{-3}$.

The contact angle results indicate incomplete wettability (Table 5). In the present study, the minimum internal bond requirements were achieved.

Table 5: Contact angle, viscosity, and solids content of the adhesives.

Adhesive	Contact Angle (°)	Viscosity (cP)	Solids Content (%)
UF	124.23	350–600	63.62

Physical and Mechanical Properties of the Panels

Panel density and compaction ratio differed significantly among treatments ($p < 0.05$), as shown in Figure 3. Density values ranged from 0.70 to $0.79\ g{\cdot}cm^{-3}$, with T3 presenting the lowest value and T4 the highest. The compaction ratio ranged from 2.69 to 2.99. No significant difference was observed between T1 and T4, whereas T3 showed significantly lower values than the other treatments.

Water absorption was significantly affected by treatment composition ($p < 0.05$), as presented in Figure 4. WA2h ranged from 40.05% to 61.49%, and WA24h ranged from 56.45% to 78.44%. T4 showed significantly

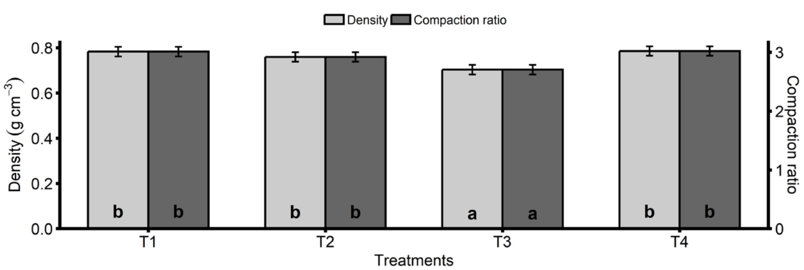

Figure 3: Apparent density (D) and compaction ratio (CR) of particleboards produced under different treatments. Error bars represent 95% confidence intervals. Different lowercase letters indicate statistically significant differences among treatments according to Tukey's test ($p < 0.05$).

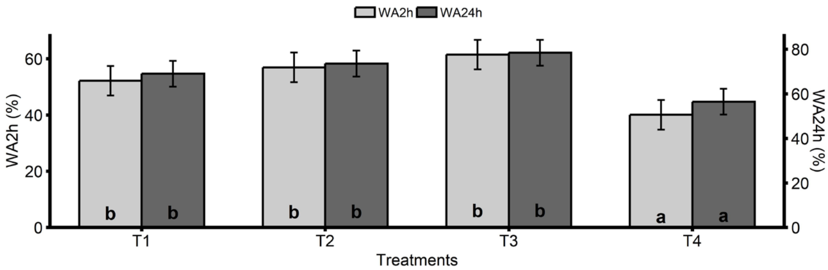

Figure 4: Water absorption after 2 h (WA2h) and 24 h (WA24h) of particleboards produced under different treatments. Error bars represent 95% confidence intervals. Different lowercase letters indicate statistically significant differences among treatments according to Tukey's test ($p < 0.05$).

lower values at both immersion times, while no significant differences were observed among T1, T2, and T3.

Thickness swelling also differed significantly among treatments ($p < 0.05$), as shown in Figure 5. TS2h ranged from 15.30% to 23.45%, and TS24h ranged from 20.96% to 29.72%. For both immersion periods, T4 presented significantly lower values than the other treatments, whereas T1, T2, and T3 did not differ statistically from each other. According to ABNT NBR 14810-2 (2024), for P2 particleboards with thickness between 13 and 20 mm, the maximum TS24h is 22%. Under this criterion, only T4 met the normative requirement.

Internal bond strength is presented in Figure 6, ranging from 0.49 to 0.80 MPa. No significant differences were observed among treatments ($p > 0.05$). All treatments exceeded the minimum requirement of 0.35 MPa established by ABNT NBR 14810-2 (2024) for P2 panels with thickness between 13 and 20 mm.

Modulus of elasticity and modulus of rupture are presented in Figure 7. MOE differed significantly among treatments ($p < 0.05$), with values ranging from 2063 to 2654 MPa. According to Tukey's test, the significant difference was observed between T2 and T3, while T1 and T4 showed intermediate values. MOR ranged from 18.6 to 23.7 MPa and did not differ significantly among treatments ($p > 0.05$). All treatments met the minimum requirements established by ABNT NBR 14810-2 (2024) for P2 panels, namely 1600 MPa for MOE and 11 MPa for MOR.

Life Cycle Inventory of the Elementary MDP Production Process

To produce 1 m^3 of MDP (12 mm thickness), specific amounts of wood, adhesive, and energy were required, as presented in Table 6. Among the evaluated treatments, CO_2e emissions ranged from 189.89 to 203.06 kg $CO_2e{\cdot}m^{-3}$, with the lowest value observed in T3 and the highest in T1.

Table 6: Life Cycle Inventory of the Elementary Production Process of MDP.

Inputs	Unit	Treatments			
		T1	T2	T3	T4
Inputs					
Wood	$kg{\cdot}m^{-3}$	361.7	359.5	344.7	375.4
Adhesive	$kg{\cdot}m^{-3}$	57.5	55.3	52.8	57.1
Energy	$MJ{\cdot}m^{-3}$	4840.9	4768.9	4649.3	4869.1
Outputs					
MDP	m^3	1.0	1.0	1.0	1.0
CO_2e (*)	$kg{\cdot}m^{-3}$	203.1	197.2	189.9	202.7

* Data obtained from Tables 7 and 8.

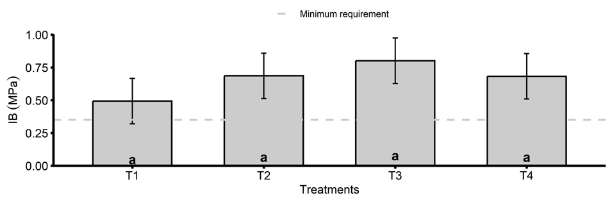

Figure 6: Internal bond strength (IB) of particleboards produced under different treatments. Error bars represent 95% confidence intervals. Different lowercase letters indicate statistically significant differences among treatments according to Tukey's test ($p < 0.05$). The dashed line indicates the minimum requirement (0.35 MPa) established by ABNT NBR 14810-2 (2024).

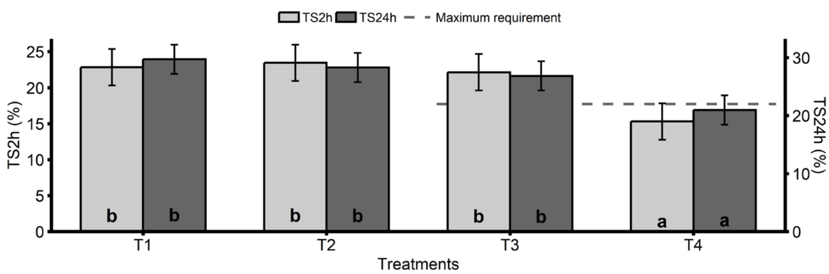

Figure 5: Thickness swelling after 2 h (TS2h) and 24 h (TS24h) of particleboards produced under different treatments. Error bars represent 95% confidence intervals. Different lowercase letters indicate statistically significant differences among treatments according to Tukey's test ($p < 0.05$).

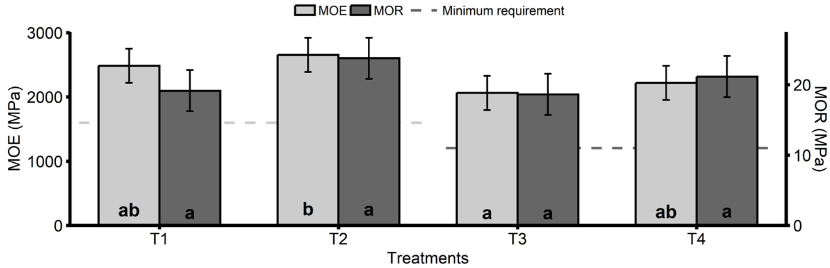

Figure 7: Modulus of elasticity (MOE) and modulus of rupture (MOR) of particleboards produced under different treatments. Error bars represent 95% confidence intervals. Different lowercase letters indicate statistically significant differences among treatments according to Tukey's test ($p < 0.05$).

The life cycle inventory was structured by disaggregating the production process into two main subsystems: forest operations and industrial processing.

The detailed distribution of energy demand among these subsystems is presented in Table 7. Forest operations showed constant energy demand across treatments (67.75 MJ·m^{-3}), whereas variations were observed within the industrial subsystem, particularly in processes such as particle generation, classification, gluing, and adhesive consumption.

The relatively high energy demand attributed to the conditioning stage reflects the prolonged environmental control required under laboratory-scale conditions. The panels remained conditioned for approximately 20 days under controlled temperature (22 ± 2 °C) and relative humidity (65 ± 5% RH), with continuous operation of the air-conditioning system throughout the conditioning period. In the present study, the total energy consumption associated with environmental conditioning was attributed to panel production. Laboratory-scale inefficiencies associated with small-scale processing and equipment operation were not individually quantified in the present inventory. Therefore, the environmental results should be interpreted as a simplified comparative assessment rather than a direct representation of industrial production efficiency.

Similarly, CO_2e emissions were distributed across the same subsystems, as shown in Table 8.

Table 7: Energy demand of particleboard production subsystems, expressed in MJ·m^{-3}, for each treatment. The system is divided into forest operations and industrial processing stages, including all unit processes involved in panel production.

Process	Energy (MJ·m^{-3})			
	T1	T2	T3	T4
Forest operations subsystem				
Wood harvesting	6.1	6.1	6.1	6.1
Log transportation	61.6	61.6	61.6	61.6
Total forest operations subsystem	67.8	67.8	67.8	67.8
Industrial subsystem				
Log conversion into billets	5.5	5.5	5.5	5.5
Billet cooking	270.5	270.5	270.5	270.5
Debarking and veneer generation	32.6	32.6	32.6	32.6
Drying	273.9	273.9	273.9	273.9
Particle generation (sliver)	300.3	298.5	286.2	311.7
Screen classification	489.4	486.4	466.4	507.9
Gluing	288.6	285.0	272.3	297.7
UF adhesive	1687.9	1624.2	1549.7	1677.1
Pre-pressing	-	-	-	-
Hot pressing	1.6	1.6	1.6	1.6
Conditioning	1322.5	1322.5	1322.5	1322.5
Panel trimming	100.5	100.5	100.5	100.5
Total industrial subsystem	4773.1	4701.1	4581.5	4801.3

Energy factors were adapted from Wilson (2010).

Table 8: CO_2e emissions of particleboard production subsystems, expressed in kg CO_2e·m^{-3}, for each treatment. The system is divided into forest operations and industrial processing stages, considering all unit processes and associated emissions.

Process	CO_2e (kg CO_2e·m^{-3})			
	T1	T2	T3	T4
Forest operations subsystem				
Wood harvesting	0.5	0.5	0.5	0.5
Log transportation	4.6	4.6	4.6	4.6
Total forest operations subsystem	5.0	5.0	5.0	5.0
Industrial subsystem				
Log conversion into billets	0.4	0.4	0.4	0.4
Billet cooking	4.1	4.1	4.1	4.1
Debarking and veneer generation	0.5	0.5	0.5	0.5
Drying	4.2	4.2	4.2	4.2
Particle generation (sliver)	4.6	4.6	4.4	4.8
Screen classification	7.5	7.4	7.1	7.7
Gluing	4.4	4.3	4.2	4.5
UF adhesive	150.7	145.0	138.4	149.8
Pre-pressing	-	-	-	-
Hot pressing	0.0	0.0	0.0	0.0
Conditioning	20.2	20.2	20.2	20.2
Panel trimming	1.5	1.5	1.5	1.5
Total industrial subsystem	198.1	192.2	184.9	197.7

Emission factors adapted from Wilson (2010).

Forest operations contributed a fixed emission value of 5.00 kg $CO_2e{\cdot}m^{-3}$, while the industrial subsystem accounted for the majority of emissions, with noticeable differences among treatments due to variations in adhesive consumption and processing steps. To facilitate visualization and comparison among treatments, the total energy demand and CO_2e emissions, as well as their contributions from each subsystem, are summarized in Figure 8.

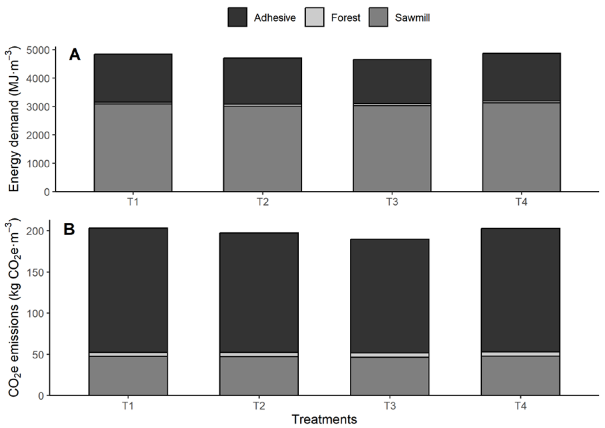

Figure 8: Energy demand (A) and CO_2e emissions (B) of particleboard production subsystems for each treatment. Bars represent the total values per treatment, partitioned into contributions from forest operations, industrial processing, and adhesive production.

DISCUSSION

Wood and Adhesive Properties

E. poeppigiana presents a chemical composition characterized by high holocellulose content and relevant levels of extractives, as reported for this species in plywood production studies (Custódio *et al.*, 2025). The predominance of holocellulose increases the availability of hydroxyl groups, resulting in higher polarity and greater affinity for water. This contributes to increased hygroscopicity and influences adhesive interaction through hydrogen bonding mechanisms.

Extractives also play an important role. In *E. poeppigiana*, they have been associated with reduced bonding efficiency due to interference with adhesive wetting and spreading (Custódio *et al.*, 2025). This limits adhesive penetration and reduces effective contact between adhesive and substrate. Similar behavior has been observed in adhesive–wood interphases, where wetting depends on surface energy and liquid–solid interaction (Amin *et al.*, 2024).

The basic density of *E. poeppigiana* is low (≈0.26–0.35 $g{\cdot}cm^{-3}$), resulting in a highly porous structure (Custódio *et al.*, 2025). This may favor adhesive penetration but increases adhesive demand due to the larger specific surface area. When adhesive content is not sufficient to cover this surface, bonding quality may be affected. This effect is related to the increase in surface-to-volume ratio, which reduces the surface-specific adhesive amount when particle size decreases (Engehausen *et al.*, 2025).

In the present study, no negative effect of viscosity on internal bond was observed. All treatments met the minimum requirement, indicating that the adhesive system presented an adequate balance between flowability and retention. Higher viscosity reduces spreading and penetration, while excessive flow reduces retention. Adhesive performance depends on the balance between these two mechanisms (Iwakiri and Trianoski, 2020; Amin *et al.*, 2024).

At the chemical level, the interaction between wood and adhesive is influenced by the relative proportion of cellulose and lignin. Cellulose favors hydrogen bonding due to its high concentration of hydroxyl groups (Klemm *et al.*, 2005), while lignin contributes to a more hydrophobic character due to its aromatic and heterogeneous structure (Lisý *et al.*, 2022). This balance affects wettability and bonding performance.

The contact angle is a key parameter to evaluate wettability and directly influences adhesive performance. Lower contact angle values indicate better spreading and penetration. Wood–adhesive interaction involves spreading, penetration into pores, and interfacial bonding (Amin *et al.*, 2024). In dynamic conditions, a decrease in contact angle over time reflects liquid absorption into the porous structure.

The effect of particle size must be interpreted considering both porosity and adhesive distribution. Fine particles reduce porosity, while coarse particles may improve mechanical performance depending on structure and mixing ratio (Chaydarreh *et al.*, 2022). However, when particle size decreases, the increase in specific surface area reduces the adhesive available per unit surface, which can negatively affect bonding (Engehausen *et al.*, 2025).

Physical and mechanical properties are also interrelated. Thickness swelling and water absorption are strongly correlated ($r = 0.7162$), while density shows a negative correlation with water absorption ($r = -0.7744$) (Mirindi *et al.*, 2025). This indicates that dimensional stability is primarily controlled by water absorption and internal structure.

The adhesive system also influences performance. Alternative adhesives can modify mechanical behavior and emission profile. For example, cardanol-based adhesives increased MOE from 764 to 1172 MPa and MOR from 2.45 to 4.39 MPa, while reducing formaldehyde emission by approximately 93% (Faria *et al.*, 2023). These results show that bonding performance depends not only on wood properties but also on adhesive chemistry.

Physical and Mechanical Properties of the Panels

Physical and mechanical properties are influenced by panel density and pressing conditions. Although ABNT NBR 14810-2 (ABNT, 2024) does not establish density as a classification criterion, the standard defines a tolerance of ±7% relative to the target density. All treatments remained within this limit, indicating adequate control of panel production.

Panel density plays a central role in board performance. Higher density reduces water absorption and thickness swelling by decreasing void volume and improving particle contact (Iswanto *et al*., 2025). This effect is associated with reduced internal porosity and limited water accessibility (Mirindi *et al*., 2025).

In the present study, density did not act as the sole controlling factor. Treatment T3 presented the lowest density and compaction ratio, with values approximately 10% lower than T1 and T4, indicating lower structural consolidation. T1, T2, and T4 showed similar density and compaction ratio values but markedly different thickness swelling behavior. Thickness swelling after 24 h was up to 41.8% higher in multilayer panels than in the single-layer configuration, while water absorption at 24 h increased by up to 38.9%. These results indicate that dimensional stability was controlled by factors beyond density, particularly internal structure and adhesive distribution.

The high compaction ratio is a direct consequence of the low basic density of *E. poeppigiana*, which requires greater particle compression during pressing. This reduces void volume but increases internal stresses. When exposed to moisture, stress release leads to thickness recovery and dimensional instability (Luan *et al*., 2022; Cabral *et al*., 2022). The high compressibility of *E. poeppigiana* can also be related to its anatomical structure, which is characterized by a high proportion of parenchymatic cells (Mesquita *et al*., 2026). These cells are composed predominantly of thin primary walls, resulting in lower mechanical resistance and facilitating particle densification during pressing. Representative tangential anatomical section of *E. poeppigiana* wood was presented in Supplementary Figure S2. This structure also contributes to higher elastic recovery when exposed to moisture, which may increase thickness swelling.

Performance is better interpreted using type P2 requirements. ABNT NBR 14810-2 (ABNT, 2024) sets a maximum thickness swelling after 24 h (TS24h) of 22%. Only T4 met this limit, while the remaining treatments exceeded it.

The lower thickness swelling observed for T4 may be associated with a more homogeneous distribution of particles and adhesive. Since no density profile or adhesive distribution analysis was performed, this interpretation should be considered as a hypothesis supported by the panel configuration and by observations reported in the literature. Multilayer panels depend on particle classification and controlled deposition. In this study, manual deposition likely resulted in non-uniform particle distribution, generating local variations in density and adhesive content. These variations may have influenced the internal structure of the panels and consequently affected dimensional stability.

As particle size decreases, the surface-to-volume ratio increases, reducing the adhesive available per unit surface area (Engehausen *et al*., 2025). This reduction may affect interparticle bonding and panel consolidation. Particle geometry also influences porosity and panel performance, with finer particles generally reducing porosity but requiring greater adhesive availability to ensure adequate bonding (Chaydarreh *et al*., 2022).

According to the literature, bonding performance may be influenced by adhesive availability and interfacial interactions. Higher binder content improves bonding quality and mechanical properties, while insufficient coverage creates discontinuities in the bonding network (Salim *et al*., 2024). These discontinuities may facilitate water absorption and reduce dimensional stability. Adhesive penetration and interfacial interaction also control bonding efficiency (Amin *et al*., 2024).

High water absorption is associated with low density and high porosity, which increase water accessibility. This relationship is well established, with strong correlation between water absorption and thickness swelling ($r = 0.7162$) and negative correlation between density and water absorption ($r = -0.7744$) (Mirindi *et al*., 2025). These results indicate that dimensional stability is primarily controlled by water absorption and internal structure.

No statistically significant differences were observed for internal bond. All treatments exceeded the minimum requirement of 0.35 MPa established by ABNT NBR 14810-2, indicating adequate bonding quality, despite a difference of approximately 62% between the lowest and highest mean values.

MOE differed among treatments ($p < 0.05$), whereas MOR did not ($p > 0.05$). MOE increased by approximately 20.4% from T3 to T1 and by 7.5% from T3 to T4, indicating the influence of structural consolidation on stiffness. This relationship is consistent with the strong correlation between mechanical properties reported in the literature, where MOR–MOE ($r = 0.8633$) and MOR–IB ($r = 0.8063$) indicate coupled mechanical behavior (Mirindi *et al*., 2025).

A similar behavior was observed for plywood produced from *E. poeppigiana*, where the incorporation of cellulose nanocrystals increased MOE by approximately 31% (from 4651 to 6076 MPa), while no significant changes were observed for MOR (Mesquita *et al*., 2026). This result reinforces that stiffness can be enhanced by modifications in the adhesive matrix without a proportional increase in strength.

All treatments exceeded the minimum values required by ABNT NBR 14810-2 (1600 MPa for MOE and 11 MPa for MOR for panels with thickness between 1.3 and 20 mm under dry conditions).

The comparison with literature (Table 9) shows that particleboards produced from *E. poeppigiana* exhibit mechanical performance comparable to or higher than several alternative raw materials, particularly in terms of MOE and MOR. Panels produced from low-density agricultural residues tend to present lower mechanical performance due to reduced structural integrity and weaker particle–adhesive interaction (Faria *et al*., 2023). In that study, MOE increased from 764 to 1172 MPa and MOR from 2.45 to 4.39 MPa with improved adhesive systems.

Panels produced with *Eucalyptus urophylla* showed lower thickness swelling and lower compaction ratios,

Table 9: Properties of particleboards from different lignocellulosic raw materials.

Raw material	Raw material density ($g \cdot cm^{-3}$)	Panel density ($g \cdot cm^{-3}$)	Compaction ratio	TS24h (%)	MOE (MPa)	MOR (MPa)	IB (MPa)
Erythrina poeppigiana[1]	0.26	0.70–0.79	2.69–2.99	20–29	2063–2654	18–23	0.49–0.80
Sugarcane bagasse[2]	—	~0.68	—	~16	~2000	~18	~0.59
Bean straw residue[3]	0.123	0.59–0.61	1.28–1.4	~20–24	611–1171	1.68–4.3	0.33–0.49
Wood–bamboo hybrid[4]	—	0.45–0.65	—	16–22	2200–4400	17–22	1.4–3.11
Pine[3]	0.477	0.61	1.27	28.8	765	2.45	0.32
Eucalyptus urophylla[5]	0.665	0.74–0.82	1.12–1.24	14–19	1434–2323	6.9–17.9	0.36–0.81

[1] This study; [2] Mesquita et al. (2019); [3] Faria et al. (2023); [4] Iswanto et al. (2025); [5] Souza et al. (2025).

indicating better dimensional stability. The higher compaction ratio observed for *E. poeppigiana* explains the increased thickness swelling, despite adequate mechanical performance.

The results indicate that panels produced with *E. poeppigiana* meet mechanical requirements for dry-use MDP. Dimensional stability remains the main limitation in multilayer configurations. The single-layer panel (T4) met the TS24h requirement, highlighting the importance of particle distribution, density uniformity, and adhesive balance.

The study evaluated only four trees and three panels per treatment, which limits material representativeness and statistical power. Density profile, anatomical characterization, and adhesive interfacial analyses were not performed. Interpretations related to adhesive distribution, internal structure, and densification behavior should therefore be considered with caution.

Energy Demand and CO_2e Emissions of the Elementary MDP Production Process

A The lower energy demand and CO_2e emissions observed for T3 are associated with its reduced consumption of wood and adhesive per declared unit, whereas T1 and T4 presented the highest environmental loads. The maximum difference in CO_2e emissions among treatments reached approximately 6.5%, indicating that variations in material consumption directly influenced the environmental profile of the panels.

Adhesive consumption was the main driver of CO_2e emissions. UF adhesive alone accounted for 138.37 to 150.72 kg $CO_2e \cdot m^{-3}$, representing approximately 72–74% of total emissions. For energy demand, UF adhesive and conditioning were the most relevant contributors. UF adhesive accounted for 1549.68 to 1687.92 $MJ \cdot m^{-3}$ (33–35%), while conditioning contributed 1322.49 $MJ \cdot m^{-3}$ (27–28%). Conditioning requires continuous thermal energy for moisture stabilization and process control. Hot pressing contributed only 1.64 $MJ \cdot m^{-3}$ and 0.025 kg $CO_2e \cdot m^{-3}$, reflecting its short duration in the production cycle.

Log transportation contributed 4.55 kg $CO_2e \cdot m^{-3}$ (2–2.5% of total emissions), while forest operations accounted for approximately 5 kg $CO_2e \cdot m^{-3}$. These contributions were minor compared to industrial processing. The panel manufacturing subsystem dominated the environmental profile, accounting for approximately 98% of total energy demand and 97–98% of CO_2e emissions.

This pattern is consistent with the LCA of MDP production in Brazil (Silva *et al*., 2013), in which the industrial stage accounted for more than 60% of impacts and approximately 92% of global warming potential. Electricity generation (34%), heavy fuel oil use (27%), and UF resin production (25%) together represented about 86% of total emissions, confirming the importance of energy and adhesive inputs.

The results obtained in the present study (190–203 kg $CO_2e \cdot m^{-3}$) are lower than those reported by Silva *et al*. (2013) (333.28 kg $CO_2e \cdot m^{-3}$), representing a reduction of approximately 39–43%. This difference is associated with lower material consumption and differences in energy inputs at the experimental scale.

Comparable values were reported in international studies. Lao and Chang (2023) estimated cradle-to-gate emissions of 348 kg $CO_2e \cdot m^{-3}$ for particleboard produced in China, while Puettmann (2022) reported values of approximately 351 kg $CO_2e \cdot m^{-3}$ for North American production. Compared with these studies, the values obtained in the present work are approximately 42–46% lower, reinforcing the influence of material efficiency and process configuration on environmental performance.

The role of carbon storage in wood-based panels should be interpreted with caution. Puettmann (2022) showed that carbon stored in wood composite panels may exceed cradle-to-gate emissions, while Wilson (2010) reported a carbon storage of −1268 kg $CO_2e \cdot m^{-3}$ for MDF.

These results highlight the importance of biogenic carbon. Direct comparison with the present study is limited by differences in product type and system boundaries.

Cangussu *et al*. (2023) reported global warming impacts of 238.79 and 330.95 kg CO_2e for particleboards produced with sugarcane bagasse and pine, respectively (per ton of raw material). The use of agricultural residues reduced impacts by approximately 28%. The authors emphasized the influence of system boundaries, allocation criteria, and transport distances on the results.

The reduction in environmental impacts observed for treatments with lower adhesive consumption agrees with previous studies, which show that the selection of alternative materials and resins improves eco-efficiency (Gavioli *et al*., 2025).

The environmental profile observed in the present study was controlled mainly by adhesive production and conditioning energy. Treatment T3 showed the lowest environmental burdens due to reduced material consumption, whereas T1 and T4 presented higher impacts due to greater demand for wood particles and UF adhesive. Material efficiency was the main factor controlling the differences among treatments.

UF adhesive was identified as the main contributor to CO_2e emissions, but the present study did not evaluate formaldehyde emissions or toxicity-related impact categories (Almeida *et al*., 2025). The environmental implications associated with UF adhesive should therefore be interpreted only from the perspective of energy demand and carbon footprint.

The use of *E. poeppigiana*, an exotic species widely employed as a shade tree in agroforestry systems, may also be associated with management strategies aimed at biodiversity enrichment. The selective removal of exotic individuals can favor the introduction or regeneration of native species, contributing to structural diversification. Although this aspect was not evaluated in the present study, it represents a potential complementary benefit of biomass utilization in agroforestry systems.

CONCLUSIONS

Particleboards produced from *E. poeppigiana* met the minimum mechanical requirements established by ABNT NBR 14810-2 (2024), confirming the technical feasibility of this species for MDP production. Dimensional stability was the main limitation. Thickness swelling exceeded the limit for P2 panels in multilayer treatments, whereas the single-layer panel (T4) met the normative requirement, indicating the influence of panel structure on performance. Panel density affected both technical and environmental results. Lower-density panels required less wood and adhesive, resulting in reduced energy demand and CO_2e emissions. Adhesive consumption was the main contributor to emissions, while the manufacturing subsystem dominated the environmental profile. The environmental performance observed in this study is directly associated with material efficiency and process configuration, particularly the use of a urea–formaldehyde adhesive representative of conventional industrial practice. Further improvements in dimensional stability are required, especially for multilayer configurations. The use of *E. poeppigiana* from agroforestry systems represents a viable alternative raw material, enabling biomass valorization without additional land-use pressure, despite the environmental impacts associated with adhesive use.

AUTHORSHIP CONTRIBUTION:

Project idea: LBSF; JAAN; RGAM
Database: LBSF; JAAN; RGAM
Processing: LBSF; JAAN; RGAM
Analysis: LBSF; JAAN; RGAM
Writing: LBSF; JAAN; RGAM; MLAV; JBGJ; LMM
Review: DP; MLAV; JBGJ; LMM

DATA AVAILABILITY:

The datasets analyzed during the current study are available from the corresponding author upon reasonable request.

REFERENCES

ALMEIDA, M. L.; GONÇALVES, F. D.; MARTINS, J. M.; et al. Addressing formaldehyde emissions in wood-based panels: evaluation of production processes, measurement strategies, and novel solutions. The Journal of Adhesion, v. 101, n. 10, p. 1252–1274, 2025. DOI: 10.1080/00218464.2024.2447718.

AMERICAN SOCIETY FOR TESTING AND MATERIALS (ASTM). ASTM D1200-10: standard test method for viscosity by Ford viscosity cup. Philadelphia, 2018.

AMERICAN SOCIETY FOR TESTING AND MATERIALS (ASTM). ASTM D1037-06: standard test methods for evaluating properties of wood-base fiber and particle panel materials. Philadelphia, 2006.

AMIN, Y.; NUGROHO, N.; BAHTIAR, E. T.; *et al*. Surface roughness, dynamic wettability, and interphase of modified melamine formaldehyde-based adhesives on jabon wood. Polymers, v. 16, n. 8, p. 1084, 2024.

ASSOCIAÇÃO BRASILEIRA DE NORMAS TÉCNICAS (ABNT). NBR 11941: madeira – determinação da densidade básica. Rio de Janeiro, 2003.

ASSOCIAÇÃO BRASILEIRA DE NORMAS TÉCNICAS (ABNT). NBR 14810-2: painéis de partículas de média densidade – parte 2: requisitos. Rio de Janeiro, 2024.

ASSOCIAÇÃO BRASILEIRA DE NORMAS TÉCNICAS (ABNT). NBR 7989: pasta celulósica e madeira: determinação de lignina insolúvel em ácido. Rio de Janeiro, 2010.

ASSOCIAÇÃO BRASILEIRA DE NORMAS TÉCNICAS (ABNT). NBR 14853: madeira – determinação do material solúvel em etanol-tolueno e em diclorometano e em acetona. Rio de Janeiro, 2010.

ASSOCIAÇÃO BRASILEIRA DE NORMAS TÉCNICAS (ABNT). NBR 13999: papel, cartão, pastas celulósicas e madeira: determinação do resíduo (cinza) após a incineração a 525 °C. Rio de Janeiro, 2017.

BRASIL. Ministério da Ciência, Tecnologia e Inovação (MCTI). Fatores de emissão de CO_2 do Sistema Interligado Nacional (SIN). Brasília, 2019.

CABEZA, L. F.; RINCON, L.; VILARINO, V.; *et al*. Life cycle assessment (LCA) and life cycle energy analysis (LCEA) of buildings and the building sector: a review. Renewable and Sustainable Energy Reviews, v. 29, p. 394–416, 2014. DOI: 10.1016/j.rser.2013.08.037.

CABRAL, J. P.; KAFLE, B.; SUBHANI, M.; *et al*. Densification of timber: a review on the process, material properties, and application. Journal of Wood Science, v. 68, p. 20, 2022. DOI: 10.1186/s10086-022-02028-3.

CANGUSSU, N.; VIEIRA, M. L. C.; MAIA, L. Environmental analysis of the incorporation of sugarcane bagasse in medium density particleboard panels through life cycle assessment. Recycling, v. 8, n. 2, p. 44, 2023. DOI: 10.3390/recycling8020044.

CHAYDARREH, K. C.; LIN, X.; GUAN, L.; *et al*. Interaction between particle size and mixing ratio on porosity and properties of tea oil camellia (Camellia oleifera Abel.) shells-based particleboard. Journal of Wood Science, v. 68, p. 43, 2022. DOI: 10.1186/s10086-022-02052-3.

CORRÊA, C. A.; TEIXEIRA, M. Z.; MATTOS, M. B. K.; *et al*. Sustainable reuse of expanded polystyrene waste in Ochroma pyramidale particle boards. International Wood Products Journal, v. 16, n. 3, p. 172–179, 2025. DOI: 10.1177/20426445251335752.

COSTA, D.; SERRA, J.; QUINTEIRO, P.; *et al*. Life cycle assessment of wood-based panels: a review. Journal of Cleaner Production, v. 444, p. 140955, 2024. DOI: 10.1016/j.jclepro.2024.140955.

CUSTÓDIO, A. P.; BORGES, I. A.; ARANTES, L. S.; *et al*. Effect of accelerated carbonation on the properties of wood cement panels from the species *Erythrina poeppigiana*. Ambiente Construído, v. 25, p. 1–14, 2025. DOI: 10.1590/s1678-86212025000100821.

EMPRESA DE PESQUISA ENERGÉTICA (EPE). Balanço energético nacional 2018: ano base 2017. Rio de Janeiro, 2018.

ENGEHAUSEN, N.; BENTHIEN, J. T.; LÜDTKE, J.; *et al*. Investigation on the influence of particle size and surface-specific adhesive amount on mechanical properties and sorption behavior of particleboard. European Journal of Wood and Wood Products, v. 83, 2025. DOI: 10.1007/s00107-025-02275-3.

FARIA, D. L.; SCATOLINO, M. V.; OLIVEIRA, J. E.; *et al*. Cardanol-based adhesive with reduced formaldehyde emission to produce particleboards with waste from bean crops. Environmental Science and Pollution Research, v. 30, p. 48270–48287, 2023. DOI: 10.1007/s11356-023-25764-5.

FARIAS, L. S.; ALMEIDA NETO, J. A.; MESQUITA, R. G. A.; *et al*. Sustainable use of *Erythrina poeppigiana* in formaldehyde-free plywood environmental and energy analysis. Ambiente Construído, v. 24, p. e132136, 2024.

GAMA-RODRIGUES, A. C.; MÜLLER, M. W.; GAMA-RODRIGUES, E. F.; *et al*. Cacao-based agroforestry systems in the Atlantic Forest and Amazon biomes: an ecoregional analysis of land use. Agricultural Systems, v. 194, p. 103270, 2021. DOI: 10.1016/j.agsy.2021.103270.

GAVIOLI, L. M.; SILVA, D. A. L.; BUENO, C.; *et al*. Life cycle assessment as a circular economy strategy to select eco-efficient raw materials for particleboard production. Resources, Conservation and Recycling, v. 212, p. 107921, 2025. DOI: 10.1016/j.resconrec.2024.107921.

INDÚSTRIA BRASILEIRA DE ÁRVORES (IBÁ). Relatório anual 2025. São Paulo, 2025. Available at: https://iba.org/wp-content/uploads/2025/10/relatorioAnual2025.pdf. Accessed in: 15 Nov. 2025.

ISWANTO, A. H.; RAJA, B. S. L.; NABILA; *et al*. Effects of board density on the properties of hybrid particleboard from kemenyan wood and belangke bamboo. IOP Conference Series: Earth and Environmental Science, v. 1445, p. 012066, 2025. DOI: 10.1088/1755-1315/1445/1/012066.

IWAKIRI, S.; TRIANOSKI, R. Painéis de madeira reconstituída. 2. ed. Curitiba: FUPEF, 2020. 259 p.

KLEMM, D.; HEUBLEIN, B.; FINK, H.; et al. Cellulose: fascinating biopolymer and sustainable raw material. Angewandte Chemie International Edition, v. 44, p. 3358–3393, 2005. DOI: 10.1002/anie.200460587..

LAO, W.; CHANG, L. Greenhouse gas footprint assessment of wood-based panel production in China. Journal of Cleaner Production, v. 389, p. 136064, 2023. DOI: 10.1016/j.jclepro.2023.136064.

LASKOWSKA, A. Characteristics of the pressing process and density profile of MUPF-bonded particleboards produced from waste plywood. Materials, v. 17, p. 850, 2024. DOI: 10.3390/ma17040850.

LISÝ, A.; HÁZ, A.; NADÁNYI, R.; *et al*. About hydrophobicity of lignin: a review of selected chemical methods for lignin valorisation in biopolymer production. Energies, v. 15, p. 6213, 2022. DOI: 10.3390/en15176213.

LOURENÇO, Y. B. C.; SANTOS, C. A.; FURTINI, A. C. C.; *et al*. Partial replacement of tannin with nanolignin in adhesive formulations for bonding plywood produced with *Erythrina poeppigiana* wood. CERNE, v. 31, n. 1, p. 1–11, 2025. DOI: 10.1590/01047760202531013546.

LUAN, Y.; FANG, C. H.; MA, Y. F.; *et al*. Wood mechanical densification: a review on processing. Materials and Manufacturing Processes, v. 37, n. 4, p. 359–371, 2022. DOI: 10.1080/10426914.2021.2016816.

MESQUITA, R. G. A.; SANADI, A. R.; MARCONCINI, J. M.; *et al*. The effect of cellulose nanocrystals in sugarcane bagasse particleboards of pith and fibers. CERNE, v. 25, n. 2, p. 203–213, 2019. DOI: 10.1590/01047760201925022621.

MESQUITA, R. G. A.; VALLE, M. L. A.; PIOTTO, D.; *et al*. The effect of cellulose nanocrystals on the properties of *Erythrina poeppigiana* (Walp.) O. F. Cook plywood. CERNE, v. 32, p. e103675, 2026.

MIRINDI, D.; SINKHONDE, D.; BEZABIH, T.; *et al*. Predictive modeling of particleboard properties derived from agricultural waste biomass using machine learning algorithms. Next Research, v. 2, p. 101045, 2025. DOI: 10.1016/j.nexres.2025.101045.

MOHD AZMAN, M. A. H.; AHMAD SOBRI, S.; NORIZAN, M. N.; *et al*. Life cycle assessment (LCA) of particleboard: investigation of the environmental parameters. Polymers, v. 13, p. 2043, 2021. DOI: 10.3390/polym13132043.

PIOTTO, D.; MARQUES, J. R. B.; NUNES, A. C. P. Desempenho de espécies madeireiras em sistema agroflorestal de cacaueiro e seringueira no sul da Bahia, Brasil. Agrotrópica, v. 32, n. 2, p. 97–104, 2020.

PUETTMANN, M. E. Carbon analysis of wood composite panels. Forest Products Journal, v. 72, n. 2, p. 112–115, 2022. DOI: 10.13073/FPJ-D-22-00010.

SALIM, R. M.; ASIK, J.; SARJADI, M. S.; *et al*. Properties of bark particleboard bonded with demethylated lignin adhesives derived from Leucaena leucocephala bark. Journal of Renewable Materials, v. 12, n. 4, 2024. DOI: 10.32604/jrm.2024.045695.

SILVA, D. A. L.; LAHR, F. A. R.; GARCIA, R. P.; *et al*. Life cycle assessment of medium density particleboard (MDP) produced in Brazil. The International Journal of Life Cycle Assessment, v. 18, p. 1404–1411, 2013.

SOUZA, M. V.; CAZELLA, P. H. S.; BISPO, R. A.; *et al*. Use of Eucalyptus urophylla waste as raw material in composite particleboards. Maderas. Ciencia y Tecnología, v. 27, n. 19, p. 1–13, 2025. DOI: 10.22320/s0718221x/2025.19.

WILSON, J. B. Life-cycle inventory of medium density fiberboard in terms of resources, emissions, energy and carbon. Wood and Fiber Science, v. 42, p. 107–124, 2010.

WORLD RESOURCES INSTITUTE (WRI); WORLD BUSINESS COUNCIL FOR SUSTAINABLE DEVELOPMENT (WBCSD). The greenhouse gas protocol: a corporate accounting and reporting standard. Washington, DC, 2022.

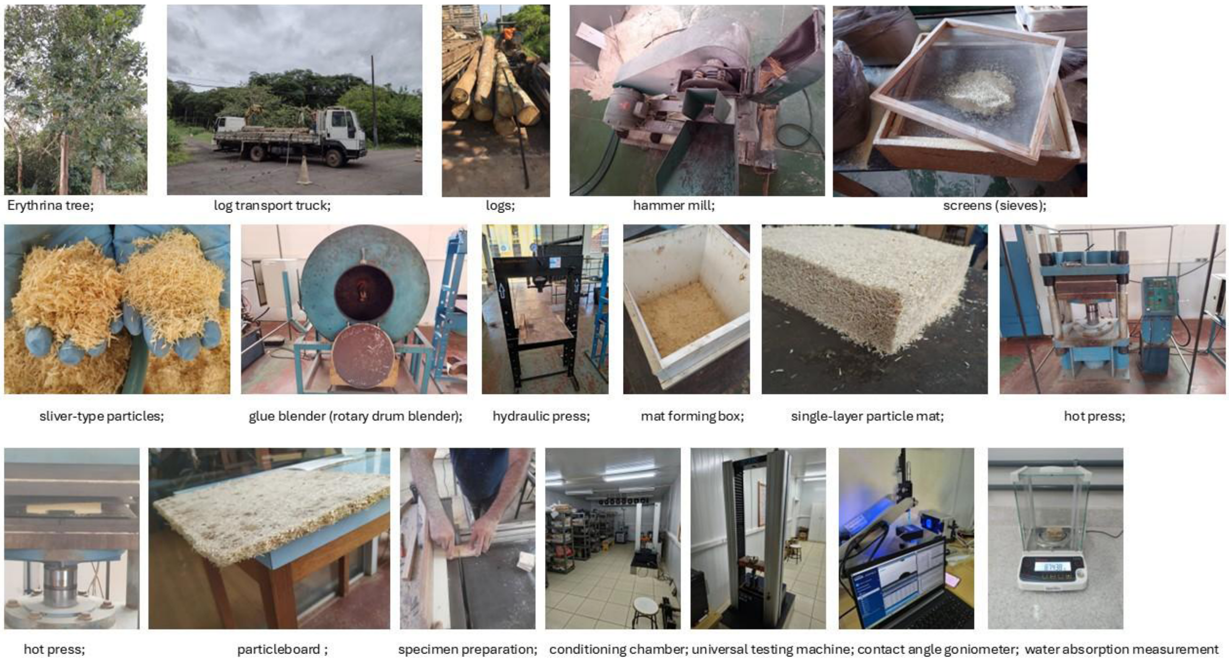

Supplementary Figure S1. Experimental procedure and equipment used for particleboard production and characterization, including wood processing, particle classification, adhesive application, mat formation, hot pressing, specimen preparation, and physical and mechanical testing.

Supplementary Figure S2. Tangential anatomical section of *Erythrina poeppigiana* wood showing abundant axial parenchyma, thin cell walls, and large lumens.